Published in final edited form as:
J Surg Res. 2012 December ; 178(2): 554–562. doi:10.1016/j.jss.2012.04.066.

Differential Calcium Handling in Two Canine Models of Right Ventricular Pressure Overload

Marc R. Moon, MD, **Abdulhameed Aziz, MD**, **Anson M. Lee, MD**, **Cynthia J. Moon, RN, CNS**, **Shoichi Okada, MD**, **Evelyn M. Kanter, BS**, and **Kathryn A. Yamada, PhD***

Division of Cardiothoracic Surgery, Washington University School of Medicine, Saint Louis, Missouri

*Department of Medicine, Washington University School of Medicine, Saint Louis, Missouri

Abstract

Background—The purpose of this study investigation was to characterize differential right atrial (RA) and ventricular (RV) molecular changes in Ca^{2+}-handling proteins consequent to RV pressure overload and hypertrophy in two common, yet distinct models of pulmonary hypertension, dehydromonocrotaline (DMCT) toxicity and pulmonary artery (PA) banding.

Materials and methods—Eighteen dogs underwent sternotomy with four groups: 1.) DMCT toxicity (n=5), 2.) mild PA banding over 10 weeks to match the RV pressure rise with DMCT (n=5), 3.) progressive PA banding to generate severe RV overload (n=4), and 4.) sternotomy only (n=4).

Results—Right Ventricle: With DMCT, there was no change in sarcoplasmic reticulum Ca^{2+}-ATPase (SERCA) or phospholamban (PLB), but a trend to downregulation of phosphorylated PLB at serine-16 (p(Ser-16)PLB) ($P = 0.07$). Similarly, with mild PA banding, there was no change in SERCA or PLB, but p(Ser-16)PLB was downregulated by 74% ($P < 0.001$). With severe PA banding, there was no change in PLB, but SERCA fell by 57% and p(Ser-16)PLB fell by 67% ($P < 0.001$). Right Atrium: With DMCT, there were no significant changes. With both mild and severe PA banding, p(Ser-16)PLB fell ($P < 0.001$), but SERCA and PLB did not change.

Conclusions—Perturbations in Ca^{2+}-handling proteins depend on the degree of RV pressure overload and the model used to mimic the RV effects of pulmonary hypertension and are similar, but blunted, in the atrium compared to the ventricle.

Keywords

right atrium; right ventricular hypertrophy; chronic pulmonary hypertension; calcium-handling proteins; dehydromonocrotaline; pulmonary banding

Address for Correspondence: Marc R. Moon, MD, Joseph C. Bancroft Professor of Surgery, Division of Cardiothoracic Surgery, Washington University School of Medicine, 660 S. Euclid Ave., Box 8234, St. Louis, Missouri 63110-1013 (314) 362-0993 FAX: (314) 747-0917, moonm@wustl.edu.

INTRODUCTION

The sarcoplasmic reticulum (SR) is an essential determinant of contraction and relaxation via its ability to regulate intracellular calcium via release during contraction and sequestration during relaxation. Calcium-handling proteins are key components of molecular remodeling associated with increased cytosolic calcium due to impaired SR calcium sequestration. The SR Ca^{2+}-ATPase isoform 2a (SERCA2a) predominates in cardiomyocytes and is a major protein involved in restoration of cytosolic calcium concentration during relaxation and is an important determinant of cardiac contractility.[1,2] Phospholamban (PLB) is the SR protein that regulates intracellular calcium homeostasis through inhibition of SERCA2a activity (19, 43).[3–5] Phosphorylation of PLB by protein kinase A at serine-16 (Ser-16) or by Ca^{2+}/calmodulin-dependent protein kinase at threonine-17 (Thr-17) reverses inhibition of SERCA2a to augment SR calcium uptake.[6–10] β-adrenergic receptor (AR) stimulation increases intracellular cAMP, promoting phosphorylation of PLB at both Ser-16 and Thr-17 to preserve calcium transport.

Alterations in Ca^{2+}-handling proteins have been identified as responsible for perturbations in left ventricular (LV) function during pressure-induced hypertrophy and cardiac failure[11–14] with chronic activation of β-AR activity.[15–17] In left-sided disease, SERCA2a inhibition contributes to diastolic and systolic dysfunction in end-stage heart failure and upregulation may improve function,[18,19] but the impact of chronic pulmonary hypertension (CPH) on right atrial (RA) and right ventricular (RV) Ca^{2+}-handling proteins remains unclear.[3,20,21] Altered levels of SERCA2a and PLB have been found in monocrotaline-treated rats, a model of CPH that produces a modest rise in RV pressure (RVP),[22] but the differential molecular adaptation in intracellular calcium homeostasis as CPH progresses from mild to severe have not been well defined.[23,24] Larsen and associates demonstrated no change in PLB or SERCA2a, but significant downregulation of phosphorylated PLB (pPLB) at Ser-16 in the right and left ventricle of chronically hypoxic mice,[25] which they theorized might be the consequence of reduced β-AR signaling. Paradoxically though, Bogaard and associates later demonstrated that β-AR blockade could reverse negative RV remodeling with CPH.[15]

The purpose of the current investigation was to characterize RA and RV molecular adaptation to varying degrees of RV pressure overload in canines using two common, yet distinct models of CPH, dehydromonocrotaline (DMCT) toxicity [26–32] and pulmonary artery (PA) banding. [3,33–35] The differential impact of these models on right heart molecular changes in Ca^{2+}-handling proteins consequent to RV pressure overload and hypertrophy has not been simultaneously assessed. Our hypothesis was that perturbations in intracellular Ca^{2+}-handling will manifest during chronic RV pressure overload with an unfavorable shift in the PLB:SERCA2a complex that depends on the degree of overload, but is independent of the mechanism of injury. In addition, directionally similar but blunted changes will manifest in the right atrium compared to the ventricle, consistent with previous studies from our laboratory and others demonstrating relatively preserved RA function to compensate for chronic RV pressure overload.[34,36–38]

MATERIALS AND METHODS

All animals received humane care in compliance with the “Principles of Laboratory Animal Care” formulated by the National Society for Medical Research and the “Guide for the Care and Use of Laboratory Animals” prepared by the National Academy of Sciences and published by the National Institutes of Health. This study was approved by the Washington University School of Medicine Animal Studies Committee and conducted according to Washington University policy.

Four groups of animals were studied: 1.) Toxic injury RV overload with DMCT (n = 5); 2.) Mild RV overload with PA banding to match the RVP rise following DMCT (n = 5); 3.) Severe RV overload with progressive PA banding to 70 to 90 mmHg (n = 4); and 4.) Sham group with placement of PA band and no RVP manipulation (n = 4).

Dehydromonocrotaline Synthesis

Dehydromonocrotaline, a well-known pulmonary endothelial toxin that causes progressive pulmonary injury, vascular remodeling, and smooth muscle hypertrophy, was used to induce CPH. Commercially available monocrotaline (Sigma-Aldrich, St. Louis, MO) was converted to toxic, bioactive DMCT as previously described (canines lack liver cytochrome oxidase to convert monocrotaline to the toxic form).[39] Purity of product was confirmed using nuclear magnetic resonance analysis.

Initial Surgical Preparation

Eighteen adult dogs (18–23 kg) were anesthetized with propofol (5–7 mg/kg), intubated, and ventilated using isoflurane (1.5–2.5%, tidal volume 10 mL/kg). After groin arterial cannulation with a fluid filled catheter to monitor arterial pressure, a warm-air cycled inflatable blanket was placed over the abdomen and lower extremities to maintain body temperature within normal limits (continuously monitored via rectal temperature probe). Canines were monitored throughout the procedure via arterial line cannulation, ECG leads, continuous pulse oximetery, and frequent arterial blood gases. Supplemental oxygen was administered as necessary to ensure adequate PaO_2 levels. Micromanometer-tipped pressure catheters (MPC-500, Millar Instruments, Inc., Houston, TX) were calibrated in a 25°C water bath for 30 minutes.

Median sternotomy was performed, leaving the pericardium intact to maintain normal RA and RV restraint, except for small incisions to permit instrumentation of the heart.[36] A 1-cm incision was made in the pericardium over the anterior RV free wall, and a 5-Fr pressure catheter was introduced through a pursestring suture. A 12-mm ultrasonic flow probe (T206 Flowmeter, Transonic Systems; Ithaca, NY) was placed around the aorta to measure cardiac output. Two additional 1-cm incisions were made in the pericardium over the RA and left atrial (LA) appendage to measure RA pressure (RAP) and LA pressure (LAP). Baseline hemodynamic data were recorded during steady-state conditions in duplicate during suspended ventilation. During each data acquisition run, ECG, RAP, LAP, RVP, and aortic flow were acquired at 200 Hz and processed using custom-designed computer software. The RVP signal was differentiated with respect to time to calculate maximum systolic pressure rise (dP/dt_{MAX}) and maximum diastolic pressure decline (dP/dt_{MIN}).

Following baseline data collection, the RV micromanometer was replaced with an indwelling 5-Fr fluid-filled pressure catheter (Access Technologies, Skokie, IL), and an inflatable silastic band (16mm diameter, Access Technologies) was secured around the main PA. The other catheters and flow probe were removed. The PA band and RVP catheter were tunneled through the chest wall, connected to reservoirs, and buried in a subcutaneous pocket. Five animals underwent RA infusion of DMCT (prepared within 24 hours of use) at 3 mg/kg dissolved in 0.1 mL//kg of dimethylformamide (solvent) to produce toxic pulmonary injury (DMCT group).[28] The sham group received saline placebo. The sternum was closed, and the animals were recovered for 7 to 10 days before any further intervention.

Subsequent Data Acquisition and Tissue Extraction

Animals underwent weekly interrogation of the RVP catheter while they were conscious and comfortable at rest. The DMCT and Sham groups had no interventions other than RVP monitoring. In the mild and severe PA banding groups, approximately one week after the

initial operation, progressive inflation of the PA band was initiated in a stepwise manner to create either mild or severe RVP overload.[34,35,37,38,40] To generate severe RV pressure overload, inflation of the PA band was performed weekly (0.3 to 0.5 mL), increasing RVP by 10 to 20 mmHg until systolic RVP reached 70 to 90 mmHg (conscious state) during the first four weeks. Pressure overload was then maintained for an additional six weeks at goal pressure. To create mild RV pressure overload, PA band inflation was performed to match the pressure elevation curves from the DMCT group (as such, it was necessary to complete all DMCT animals before initiating the mild PA band group). The target RVP for mild PA banding was elevation to 35 mmHg by week 2 and 40 mmHg by week 4, then maintaining inflation for an additional 6 weeks at goal pressure. Occasionally, when intermittent or permanent catheter thrombosis precluded adequate RVP measurement, two-dimensional echocardiography was performed to quantify RVP. Echocardiography was also performed at baseline and at 10 weeks in all animals to quantify RV and LV mass using Simpson's rule, assuming myocardial tissue density of 1.05 gm/mL.[41] Midventricular RV free wall thickness and cross sectional area were also measured to yield fractional area shortening (to quantify contractility) and end-systolic RV wall stress = (RVP × RV internal diameter)/(2 × wall thickness) × 1.332 (k×dynes/cm^2).

After 10 weeks (76 ± 16 days), animals were anesthetized as described above and underwent redo sternotomy. Micromanometer-tipped catheters and a flow probe were again inserted, and hemodynamic data were acquired in duplicate during suspended ventilation. Following data collection, the azygous vein and vena cavae were ligated, and the right inferior pulmonary vein and inferior vena cava were expeditiously vented before aortic cross-clamping and infusion of 400 mL Lactated Ringer's with potassium chloride into the aortic root to arrest the heart. Frozen Lactated Ringer's slush was placed in the chest to further expedite arrest and tissue preservation. Following arrest, 100 mL of Lactated Ringer's with 1 mL protease inhibitor cocktail (Sigma-Aldrich, St. Louis, MO) was infused for protein preservation. The heart was excised, the right atrium and ventricle were each divided into 5 horizontal sections and cut into 1 cm vertical intervals, then snap frozen in liquid nitrogen and stored at −80°C.

Protein Immunoblot Analysis

To prepare extracts, flash frozen samples were pulverized, homogenized in tissue extraction reagent (TPER, Pierce Chemical Co., Rockford, IL) containing a protease inhibitor cocktail (Thermo Scientific, Inc., Waltham, MA) and phosphatase inhibitor cocktail (Sigma-Aldrich, Saint Louis, MO) and sonicated. Protein content was measured using the Coomassie Plus (Pierce) assay, and 10–30 μg aliquots of protein were resolved by SDS-PAGE on 4–12% NuPage Bis-Tris gradient gels using a MOPS buffer system and SeeBlue Plus2 as the standard (Invitrogen, Carlsbad, CA) or 8% or 15% gels using SDS-Tris buffer and run against a Color Plus prestained broad range protein marker (New England BioLabs, Inc., Ipswich, MA). Resolved proteins were then transferred electrophoretically to nitrocellulose membranes (Invitrogen) and blocked in 2% bovine serum albumin, 3% nonfat dry milk in Tris-buffered saline–0.1% Tween 20. The membranes were incubated for either two hour at room temperature or 16 hours overnight at 4°C using antibodies directed against SERCA2a (product #MA3-919, Thermo Scientific/Pierce Biotechnology, Rockford, IL), PLB (product #ab2865, Abcam Inc., Cambridge, MA), and p(Ser-16)PLB (product # sc-12963-R) and p(Thr-17)PLB (product #sc-17024-R, Santa Cruz Biotechnology, Inc., Santa Cruz, CA). Three ten-lane gels were required for each antibody to analyze all 18 animals. Protein bands were visualized using Western Lightning Plus-ECL (PerkinElmer Inc, Waltham, MA). The membranes were stripped and reblotted with specific antibodies against glucose-6-phosphate dehydrogenase (GAPDH, product #10R-G109A, Fitzgerald Intl, Concord, MA), which

served as loading control. The resulting blots were digitized and quantified by densitometric analysis with Adobe Photoshop.

Statistical Analysis

All continuous data are reported as mean ± standard deviation. Ventricular mass and steady-state hemodynamic data obtained during baseline and at 10 weeks (average five beats in duplicate) were compared using two-way repeated measures analysis of variance (ANOVA) and Fisher's protected least significant difference (LSD) test. Calcium-handling protein data, which was obtained only at the terminal study, were compared using one-way ANOVA and Fischer's LSD test. Linear regression analysis was calculated with 95% confidence intervals. Statistical analyses were performed using SigmaStat (2.03 SPSS Inc., Chicago, IL). Differences were considered significant at a level of $P < 0.05$.

RESULTS

Creation of chronic RV pressure overload

Figure 1 summarizes mean weekly systolic RVP for all four groups measured in a conscious, spontaneously breathing state. There was persistent elevation of RVP beyond week three in the DMCT and PA band groups but not the Sham group, with the most substantial rise with severe PA banding. In all RVP overload groups, increased pressure resulted in RV hypertrophy (increased RV mass) versus Sham (Figure 2A). RV mass normalized to body weight (mg/kg) increased by 30% in DMCT (1.60 ± 0.48 to 2.08 ± 0.69, $P = 0.04$), 50% in mild PA banding (1.50 ± 0.31 to 2.24 ± 0.59, $P = 0.01$), and 69% in severe PA banding (1.16 ± 0.23 to 1.95 ± 0.40, $P = 0.02$). There was no significant change in RV mass in the Sham group (1.46 ± 0.48 to 1.75 ± 0.67, $P = 0.34$) and no change in LV mass in any group ($P > 0.18$ for all) (Figure 2B).

Hemodynamics changes

Table 1 summarizes the steady-state hemodynamic data in all four groups. Baseline data were pooled in Table 1 for ease of presentation, but statistical analyses were performed using group-specific baselines. These data were obtained in an open-chest, closed-pericardium, anesthetized state at Baseline and at 10 weeks. In the Sham group, there was no change in maximum RVP ($P = 0.88$), mean RAP ($P = 0.19$), mean LAP ($P = 0.54$) or cardiac output ($P = 0.76$). In the severe PA band group, RVP rose by 97% ($P < 0.001$), RAP rose by 63% ($P = 0.001$), but LAP ($P = 0.21$) and CO ($P = 0.68$) did not change. Similarly, right-sided pressures rose with DMCT and mild PA banding, but to a lesser degree than with severe PA banding. There was no significant change in RV force generation or diastolic recoil rate as quantified by RV dP/dt_{MAX} and RV dP/dt_{MIN} in any group ($P = 0.10$ and $P = 0.19$, respectively). There was a significant increase in RV free wall thickness with mild ($P = 0.03$) and severe ($P = 0.02$) PA banding but no change with DMCT ($P = 0.52$) or sham ($P = 0.89$). There was no change in RV fractional area shortening in any group ($P > 0.52$ for all), but while end-systolic RV wall stress did not change in sham ($P = 0.87$), DCMT ($P = 0.54$), or mild PA banding ($P = 0.18$), it more than doubled in the severe PA band group ($P = 0.005$).

Right ventricular Ca^{2+}-handling proteins

Table 2 summarizes changes in RV Ca^{2+}-handling proteins normalized to the sham-operated control group. In the right ventricle, with DMCT, there was no change in SERCA2a ($P = 0.50$) or PLB ($P = 0.42$). Similarly, with mild PA band, there was no significant change in SERCA2a ($P = 0.25$) or PLB ($P = 0.33$). With severe PA band, there was no change in PLB ($P = 0.33$) but SERCA2a fell by 67% ($P < 0.004$). Figure 3 illustrates Western blot analysis

for SERCA2a and PLB. RV SERCA2a fell with severe PA band, but RV PLB did not change in any RVP overload group (Table 2). The RV PLB:SERCA2a protein ratio was significantly elevated in severe PA band ($P = 0.01$) but not DMCT or mild PA band (Figure 4). Plotting RV PLB:SERCA2a protein ratio against the corresponding systolic RVP (anesthetized, open-chest) of all 18 animals indicated a moderate correlation ($r = 0.65$, $r^2 = 0.42$, $P = 0.004$) between the ratio of Ca^{2+}-handling proteins and pressure loading (PLB:SERCA2a = −0.22 + (0.47 × RVP)) (Figure 5).

Examining site-specific phosphorylation of PLB in the right ventricle, with DMCT, there was a trend toward reduced p(Ser-16)PLB ($P = 0.07$) (Table 2). With PA band, p(Ser-16)PLB fell in both the mild and severe groups by 74% ($P < 0.001$) and 67% ($P < 0.001$), respectively. There was a significant decline in the p(Ser-16)PLB:PLB protein ratio from sham (1.02 ± 0.22) in all three groups: DMCT fell to 0.69 ± 0.24 ($P = 0.05$), mild PA band fell to 0.32 ± 0.46 ($P = 0.03$), and severe PA band fell to 0.39 ± 0.29 ($P = 0.01$). With both mild and severe PA band, phosphorylation of PLB also fell at the Thr-17 amino acid residues by 37% ($P = 0.05$) and 30% ($P = 0.02$), respectively. Figure 6 demonstrates Western blot analysis of site-specific phosphorylation of PLB at Ser-17 and Thr-17. Figure 7 demonstrates a tendency for pPLB to fall at both Ser-16 and Thr-17 in all three RVP overload groups.

Right atrial Ca^{2+}-handling proteins

Table 2 summarizes changes in RA Ca^{2+}-handling proteins normalized to the sham operated control group. In the right atrium, changes in Ca^{2+}-handling proteins were blunted compared to the right ventricle in all RVP overload groups. There was no significant change in RA SERCA2a ($P = 0.68$) or PLB ($P = 0.31$) in any group, and the RA PLB:SERCA2a protein ratio, unlike in the right ventricle, remained near unity in all groups ($P = 0.96$) (Figure 4).

Examining site-specific phosphorylation of PLB in the right atrium, with DMCT, pPLB did not significantly change at Ser-16 ($P = 0.41$) or Thr-17 ($P = 0.40$) (Table 2). With mild PA band, RA pPLB fell by 60% at Ser-16 ($P < 0.001$) but did not change at Thr-17 ($P = 0.59$). With severe PA band, RA pPLB fell by 63% at Ser-16 compared to control ($P < 0.001$) and by 42% at Thr-17 ($P = 0.04$). Figure 8 demonstrates a fall in p(Ser-16)PLB with mild and severe PA band, but a fall in p(Thr-17)PLB in only the severe PA band group.

DISCUSSION

In the current report, we found differential changes in Ca^{2+}-handling proteins depending on the degree of RV overload and heterogeneity between right heart chambers. In the right ventricle, PLB did not change, SERCA2a fell only with severe PA banding, but PLB phosphorylation was downregulated in most groups. In the right atrium, changes in Ca^{2+}-handling proteins were blunted, but diminished PLB phosphorylation was present with both mild and severe PA banding.

Previous investigators have demonstrated that severe compensated hypertrophy and cardiac failure secondary to pressure overload is accompanied by a large fall in SERCA mRNA and proteins.[1,42,43] Diminished SERCA is associated with diminished calcium uptake, but with acute pressure overload, SERCA can be upregulated. In a rat model of LV hypertrophy (aortic constriction), at day 1, SERCA was 60–80% higher than normal, at day 5, SERCA levels were at baseline, but at 1 month, SERCA had fallen by 40–60%.[1] The early rise in SERCA may be a reflection of nonspecific global stimulation of the cardiac genome in acute stress, while late changes may represent a compensatory response to prolonged overload.[21,44] In the current report, we did not assess Ca^{2+}-handling proteins during acute PA hypertension, but with mild CPH, there was no change in SERCA or PLB levels. In

contrast, with severe PA banding, SERCA levels fell by 67%, consistent with the 60% decline in the aortic constriction model of Anger and colleagues,[1] and there was a similar directional change in the right atrium but to a lesser degree.

Gupta and associates found that PA banding has an adverse impact on the expression of Ca^{2+}-handling proteins in the right atrium.[3] Following 10 weeks of PA banding in rabbits producing a 30% rise in RA weight, RA SERCA fell by 55% but PLB and pPLB did not change. In the current report, there was no change in RA SERCA2a or PLB in canines, but there was a substantial decrease in pPLB and there was no loss of contractile function. Previous hemodynamic studies from our laboratory have demonstrated enhanced RA and RV elastance with PA banding, but a fall in RV diastolic compliance and RV circumferential and minimum principal strain.[34,37] Verhaert and colleagues also noted diminished RV strain in decompensated heart failure.[45] In the current report, both the right atrium and ventricles were affected, but to varying degrees. There was downregulation of SERCA2a in the ventricle only, while pPLB fell in both chambers. The current finding of a decline in p(Ser-16)PLB and p(Thr-17)PLB suggests a similar directional change in PLB:SERCA2a coupling (an increase in this relationship impairs calcium transport), as the result of diminished reversal of PLB inhibition.

Larsen and associates found that chronic alveolar hypoxia induced hypophosphorylation of PLB at Ser-16, thought secondary to diminished β-AR signaling.[25] The Virginia Commonwealth University group has also done extensive experimentation with a combined hypoxia and vascular endothelial growth factor (VEGF) receptor blockade model to produce CPH.[15,46,47] Their work has demonstrated that while β-AR blockade with Caredilol did not alter the morphology or the pulmonary vessels or RV afterload, it increased protein kinase G activity and improved RV function with RV fetal gene reactivation.[15] They later went on to identify the molecular signature of RV failure in CPH with loss of genes promoting cell growth, impairment of angiogenic capillary maintenance and elevated glycolytic enzymes, with a phenotypic negative RV remodeling response that was attenuated by tumor suppressor p53 gene.[46,47]

Early in the development of CPH, contractility is preserved, potentially at the expense of diastolic relaxation. Muller and coauthors found that diastolic function was impaired in CPH but, in transgenic rats with SERCA overexpression, relaxation was preserved and directly related to SERCA concentration.[13] In the current report, there was a modest, but potentially interesting correlation between the PLB:SERCA2a ratio and the degree of RV pressure loading. As systolic RVP increased, the PLB:SERCA2a complex favored PLB dephosphorylation. Muller's study did not address the potentially maladaptive decline in pPLB that we identified with higher degrees of RV overload in the current report. We hypothesize that the PLB:SERCA2a complex and PLB phosphorylation are at the center of the RA and RV response to chronic overload, such that overexpression or underexpression of either component of the ratio will modulate the negative response.

Weber and co-investigators investigated the mechanism responsible for diminished phosphorylation of PLB in acute LV ischemia by examining the balance between reduced phosphorylation and increased dephosphorylation.[9] They noted no change in enzyme activity and concluded that in myocardial stunning, decreased intracellular cAMP, consequent to a fall in β-AR density or enhanced degradation of cAMP, represents the initial event leading to altered Ca^{2+}-handling, impaired relaxation, and contractile dysfunction. In the current report, we identified similar changes in PLB site-specific phosphorylation with a fall in p(Ser-16)PLB and p(Thr-17)PLB during both mild and severe RV overload. Future studies will be necessary to investigate potential mechanisms which include: decreased β-AR density/function or decreased adenyl cyclase activity, increased cAMP degradation,

diminished protein kinase A activity (less phosphorylation of PLB at Ser-16) and diminished Ca^{2+}/calmodulin-dependent protein kinase II activity (less phosphorylation of PLB at Thr-17), or increased phosphatase activity.[9]

Based on the findings of the current report, our working hypothesis for future studies is that enhanced Ca^{2+}-handling (i.e., SERCA overexpression) can partially rescue the right heart, whereas a decrease in SERCA at baseline will aggravate the negative impact of CPH on RA and RV mechanics. Although heart failure is associated with a reduction in SERCA activity and calcium uptake, attempts to reverse these negative changes have demonstrated only transient improvements in function. Molina and colleagues demonstrated that adenovirus-mediated SERCA gene transfer and β-AR kinase 1 inhibitor enhanced RV Ca^{2+}-handling and improved contractility in an aortic constriction model of biventricular failure, although the beneficial changes were, for the most part, transient.[16,17] In addition, these changes may have been upstream changes secondary to diminished phenotypic severity of LV dysfunction; i.e., intracoronary β-AR kinase 1 inhibitor in LV overload improved LV function and, as a consequence, improved RV function. The present data provide evidence for alterations of calcium homeostasis in RV pressure overload. Decreased SERCA and decreased phosphorylation of PLB may contribute to impaired relaxation and diastolic dysfunction that has been demonstrated in previous functional studies.[28,34] It has been our contention that the right atrium plays a compensatory role during RV pressure overload to maintain RV filling with blunted negative changes compared to the ventricle.[34,37]

Potential limitations

In this study, we used two models that mimic CPH at the hemodynamic level (chronic RV pressure overload with PA banding) and cellular level in the pulmonary vasculature (chemically-induced CPH with DMCT toxicity). We feel, as others have suggested, that both models are relevant to CPH and each has specific advantages.[30,33,48] Neuroendocrine factors are not sufficient to alter RV molecular mechanics in CPH, rather enhanced biomechanical loading conditions are necessary to induce the hypertrophic RV phenotype typical of chronic, severe pulmonary vasoconstrictive disorders.[33] While chronic RV pressure overload does not mimic CPH in the lungs, the functional, biomechanical, and molecular consequences on the right heart are clinically relevant to both primary and secondary CPH in humans, and a substantial degree of CPH with RV dysfunction can be achieved. In contrast, toxic exposure more directly mimics the pulmonary vascular changes seen in primary pulmonary hypertension; however, the degree of CPH in canines is relatively modest and generally does not produce clinical RHF in large animals and is not ideal to mimic human forms of severe plexogenic CPH, which is our ultimate translational goal.[31,32] We feel strongly that this combined approach creates a fertile opportunity to evaluate the biomechanical and molecular mechanisms of CPH, RV dysfunction, and its treatment. The models of RV dysfunction in the current study do not produce severe RV failure to the degree seen with combined hypoxia and vascular endothelial growth factor (VEGF) receptor blockade.[15,30,46,47,49,50] The more angioproliferative model can induce severe RV failure that mimics human RV failure and has yielded important clinical results in small animals. However, the hypoxia methods are impractical in the large animal models necessary to perform right atrial strain and function analyses which have been a part of our overall investigation during the last decade,[34,36–38,40] but we plan to consider their use in future studies involving mechanistic investigation of PLB site-specific phosphorylation and molecular interventions.

Another potential limitation is that the relatively small number of animals used in each group could have resulted in a type I error. However, the findings were quite consistent between animals, and we feel that the statistics were sufficient to support the conclusions. As such, it would not have been cost-effective to include more animals. In addition, ideally

animals would have been placed in one of the study groups randomly, but the DMCT animals were all completed before the PA banding groups were initiated. While our laboratory was very familiar with the anticipated weekly pressure rise with severe PA banding, we had to perform the DMCT studies first to allow pressure elevation matching in the mild PA banding group. Furthermore, baseline and terminal hemodynamic measurements were made in open-chest, anesthetized animals, which is a limitation in that it can impact chamber pressures, but we were careful to leave the pericardium intact, which we have previously shown is most important factor for right heart measurements.[36] Finally, our study investigated the upstream changes in RA and RV molecular mechanisms, rather than addressing the primary inciting events that occur in the pulmonary vasculature as others have done.[30,44,50]

In summary, the current study demonstrated that perturbations in Ca^{2+}-handling proteins depend on the degree of RV pressure overload and the model used to mimic the RV effects of pulmonary hypertension and are similar, but blunted, in the right atrium compared to the right ventricle. Right heart dysfunction that occurs with CPH, whether due to RV pressure overload or toxic exposure, is associated with diminished SERCA2a expression and PLB dephosphorylation. Measures to increase SERCA2a or augment phosphorylation of PLB may ameliorate detrimental pathologic changes and augment the compensatory RA response to chronic RV pressure overload.

Acknowledgments

This study was supported by National Heart, Lung, and Blood Institute Grants R01 HL-92088 and T32-HL-07776 (to A. Aziz and A.M. Lee). We gratefully acknowledge Nneka N. Ufere, BA, who was supported by a Research Scholarship from the American Association for Thoracic Surgery, Noel J. Bernabe, Jr., P. Diane Toeniskoetter, and Naomi R. Still for their technical assistance, Zhenfu Han, PhD for biochemistry assistance, and Richard B. Schuessler, PhD for assistance with study design.

References

1. Anger M, Lompre A, Vallot O, Marotte F, Rappaport L, Samuel J. Cellular distribution of Ca^{2+} pumps and Ca^{2+} release channels in rat cardiac hypertrophy induced by aortic stenosis. Circulation. 1998; 98:2477. [PubMed: 9832495]
2. Huke S, Liu LH, Biniakiewicz, Abraham WT, Periasamy M. Altered force-frequency response in non-failing hearts with decreased SERCA pump-level. Cardiovasc Res. 2003; 59:668. [PubMed: 14499868]
3. Gupta SC, Varian KD, Bal NC, Abraham JL, Periasamy M, Janssen PML. Pulmonary artery banding alters the expression of Ca^{2+} transport proteins in the right atrium in rabbits. Am J Physiol Heart Circ Physiol. 2009; 296:H1933. [PubMed: 19376811]
4. Sano M, Minamino T, Toko H, Miyauchi H, Orimo M, Qin Y, Akazawa H, Tateno K, Kayama Y, Harada M, Shimizu I, Asahara T, Hamada H, Tomita S, Molkentin JD, Zou Y, Komuro I. p53-induced inhibition of Hig-1 causes cardiac dysfunction during pressure overload. Nature. 2007; 446:444. [PubMed: 17334357]
5. Shanmugam M, Gao S, Hong C, Fefelova N, Nowycky MC, Xie LH, Periasamy M, Babu GJ. Ablation of phospholamban and sarcolipin results in cardiac hypertrophy and decreased cardiac contractility. Cardiovasc Res. 2011; 89:353. [PubMed: 20833651]
6. Boknik P, Unkel C, Kirchhefer U, Kleideiter U, Klein-Wiele O, Knapp J, Linck B, Luss H, Muller FU, Schmitz W, Vahlensieck U, Zimmermann N, Jones LR, Neumann J. Regional expression of phospholamban in the human heart. Cardiovasc Res. 1999; 43:67. [PubMed: 10536691]
7. Lindemann JP, Jones LR, Hathaway DR, Henry BG, Watanabe AM. β-adrenergic stimulation of phospholamban phosphorylation and Ca^{2+}-ATPase activity in guinea pig ventricles. J Biol Chem. 1983; 258:464. [PubMed: 6217205]

8. Luss I, Boknik P, Jones LR, Kirchhefer U, Knapp J, Linck B, Luss H, Meissner A, Muller FU, Schmitz W, Vahlensieck U, Neumann J. Expression of cardiac calcium regulatory proteins in atrium v ventricle in different species. J Mol Cell Cardiol. 1999; 31:1299. [PubMed: 10371704]
9. Weber T, Neumann J, Meibner A, Hartlage MG, Aken HV, Hanske G, Schmitz W, Boknik P. Reduced serine-16 and threonine-17 phospholamban phosphorylation in stunning of conscious dogs. Basic Res Cardiol. 2006; 101:253. [PubMed: 16369730]
10. Dieterle T, Meyer M, Gu Y, Belke DD, Swanson E, Iwatate M, Hollander J, Peterson KL, Ross J Jr, Dillmann WH. Gene transfer of a phospholamban-targeted antibody improves calcium handling and cardiac function in heart failure. Cardiovasc Res. 2005; 67:678. [PubMed: 15927173]
11. Hasenfuss G, Reinecke H, Studer R, Meyer M, Pieske B, Holtz J, Holubarsch C, Posival H, Just H, Drexler H. Relation between myocardial function and expression of sarcoplasmic reticulum Ca^{2+}-ATPase in failing and nonfailing human myocardium. Circ Res. 1994; 75:434. [PubMed: 8062417]
12. Kiss E, Ball NA, Kranias EG, Walsh RA. Differential changes in cardiac phospholamban and sarcoplasmic reticular Ca^{2+}-ATPase protein levels. Effects on Ca^{2+} transport and mechanics in compensated pressure-overload hypertrophy and congestive heart failure. Circ Res. 1995; 77:759. [PubMed: 7554123]
13. Muller OJ, Lange M, Rattunde H, Lorenzen H, Muller M, Frey N, Bittner C, Simonides W, Katus HA, Franz W. Transgenic rat hearts overexpressing SERCA2a show improved contractility under baseline conditions and pressure overload. Cardiovasc Res. 2003; 59:380. [PubMed: 12909321]
14. Sande JB, Sjaastad I, Hoen IB, Bokenes J, Tonnessen T, Holt E, Lunde PK, Christensen G. Reduced level of serine(16) phosphorylated phospholamban in the failing rat myocardium: a major contributor to reduced SERCA2 activity. Cardiovasc Res. 2002; 53:382. [PubMed: 11827689]
15. Bogaard HJ, Natarajan R, Mizuno S, Abbate A, Change PJ, Chau VQ, Hoke NN, Kraskauskas D, Kasper M, Salloum FN, Voelkel NF. Adrenergic receptor blockade reverses right heart remodeling and dysfunction in pulmonary hypertensive rats. Am J Respir Crit Care Med. 2010; 182:652. [PubMed: 20508210]
16. Molina EJ, Gupta D, Palma J, Gaughan JP, Macha M. Right ventricular beneficial effects of beta adrenergic receptor kinase inhibitor (βARKct) gene transfer in a rat model of severe pressure overload. Biomed Pharmacother. 2009; 63:331. [PubMed: 18801641]
17. Molina EJ, Gupta D, Palma J, Gaughan JP, Macha M. Right ventricular beneficial effects of intracoronary SERCA2a gene transfer in an experimental model of heart failure. Folia Biol (Praha). 2010; 56:1. [PubMed: 20163775]
18. Currie S, Smith GL. Enhanced phosphorylation of phospholamban and downregulation of sarco/endoplasmic reticulum Ca^{2+} ATPase type 2 (SERCA 2) in cardiac sarcoplasmic reticulum from rabbits with heart failure. Cardiovasc Res. 1999; 41:135. [PubMed: 10325961]
19. Maier LS, Wahl-Schott C, Horn W, Weichert S, Pagel C, Wagner S, Dybkova N, Müller OJ, Näbauer M, Franz WM, Pieske B. Increased SR Ca^{2+} cycling contributes to improved contractile performance in SERCA2a-overexpressing transgenic rats. Cardiovasc Res. 2005; 67:636. [PubMed: 15932750]
20. Hiranandani N, Bupha-Intr T, Janssen PML. SERCA overexpression reduces hydroxyl radical injury in murine myocardium. Am J Physiol Heart Circ Physiol. 2006; 291:H3130. [PubMed: 16798816]
21. Roncon-Albuquerque R, Vasconcelos M, Lourenco AP, Brandao-Nogueira A, Teles A, Henriques-Coelho, Leite-Moreira AF. Acute changes of biventricular gene expression in volume and right ventricular pressure overload. Life Sci. 2006; 78:2633. [PubMed: 16310223]
22. Seyfarth T, Gerbershagen HP, Giessler C, LEineweber K, Heinroth-Hoffmann I, Ponicke K, Brodde OE. The cardiac β-adrenoreceptor-G-protein(s)-adenylyl cyclase system in monocrotaline-treated rats. J Mol Cell Cardiol. 2000; 32:2315. [PubMed: 11113007]
23. Bogaard HJ, Abe K, Noordegraaf AV, Voelkel NF. The right ventricle under pressure. Cellular and molecular mechanisms of right-heart failure in pulmonary hypertension. Chest. 2009; 135:794. [PubMed: 19265089]

24. Pasipoularides A, Shu M, Shah A, Silvestry S, Glower DD. Right ventricular diastolic function in canine models of pressure overload, volume overload, and ischemia. Am J Physiol Heart Circ Physiol. 2002; 283:H2140. [PubMed: 12384492]
25. Larsen KO, Sjaastad I, Svinndland A, Krobert KA, Skjonsberg OH, Christensen G. Alveolar hypoxia induces left ventricular diastolic dysfunction and reduces phosphorylation of phospholamban in mice. Am J Physiol Heart Circ Physiol. 2006; 291:H507. [PubMed: 16582020]
26. Chen EP, Craig DM, Bittner HB, Davis RD, Van Trigt P 3rd. Pharmacological strategies for improving diastolic dysfunction in the setting of chronic pulmonary hypertension. Circulation. 1998; 97:1606. [PubMed: 9593566]
27. Chen EP, Akhter SA, Bittner HB, Koch WJ, Davis RD, Van Trigt P 3rd. Molecular and functional mechanisms of right ventricular adaptation in chronic pulmonary hypertension. Ann Thorac Surg. 1999; 67:1053. [PubMed: 10320250]
28. Gust R, Schuster DP. Vascular remodeling in experimentally induced subacute canine pulmonary hypertension. Exp Lung Res. 2001; 27:1. [PubMed: 11202060]
29. Lovoulos C, Tittle S, Goldstein L, Austin D, Singh S, Rocco E, Keane J, Tang P, Kopf GS, Elefteriades JA. Right ventricle-sparing heart transplantation effective against iatrogenic pulmonary hypertension. J Heart Lung Transplant. 2004; 23:236. [PubMed: 14761772]
30. Stenmark KR, Meyrick B, Galie N, Mooi WJ, McMurtry IF. Animal models of pulmonary arterial hypertension: the hope for etiological discovery and pharmacological cure. Am J Physiol Lung Cell Mol Physiol. 2009; 297:L1013. [PubMed: 19748998]
31. Gomez-Arroyo JG, Farkas L, Alhussaini AA, Farkas D, Kraskauskas D, Voelkel NF, Bogaard HJ. The monocrotaline model of pulmonary hypertension in perspective. Am J Physiol Lung Cell Mol Physiol. 2012; 302:L363. [PubMed: 21964406]
32. Gomez-Arroyo JG, Saleem SJ, Mizuno S, Syded AA, Bogaard HJ, Abbate A, Taraseviciene-Stewart L, Sung Y, Kraskauskas D, Farkas D, Conrad DH, Nicolls MR, Voelkel NF. A Brief Overview of Mouse Models of Pulmonary Arterial Hypertension: Problems and Prospects. Am J Physiol Lung Cell Mol Physiol. 2012 Feb 3. [Epub ahead of print].
33. Calvin JE, Baer RW, Glantz SA. Pulmonary artery constriction produces a greater RV dynamic afterload than lung microvascular injury in the open chest dog. Circ Res. 1985; 56:40. [PubMed: 3881198]
34. Gaynor SL, Maniar HS, Bloch JB, Steendijk P, Moon MR. Right atrial and ventricular adaptation to chronic right ventricular pressure overload. Circulation. 2005; 112(Suppl I):I-212. [PubMed: 16159819]
35. Hsieh CM, Mishkel GJ, Cardoso PFG, Rakowski H, Dunn SC, Butany J, Weisel RD, Patterson GA. Production and reversibility of right ventricular hypertrophy and right heart failure in dogs. Ann Thorac Surg. 1992; 54:104. [PubMed: 1535190]
36. Maniar HS, Prasad SM, Gaynor SL, Chu CM, Steendijk P, Moon MR. Impact of pericardial restraint on right atrial mechanics during acute right ventricular pressure load. Am J Physiol Heart Circ Physiol. 2003; 284:H350. [PubMed: 12388317]
37. Voeller RK, Aziz A, Maniar HS, Ufere NN, Taggar AK, Bernabe NJ Jr, Cupps BP, Moon MR. Differential modulation of right ventricular strain and right atrial mechanics in mild versus severe pressure overload. Am J Physiol Heart Circ Physiol. 2011; 301:H2362. [PubMed: 21926343]
38. Zierer A, Voeller RK, Melby SJ, Steendijk P, Moon MR. Impact of calcium-channel blockers on right heart function in a controlled model of chronic pulmonary hypertension. Eur J Anaesthesiol. 2009; 26:253. [PubMed: 19237986]
39. Mattocks AR, Jukes R, Brown J. Simple procedures for preparing putative toxic metabolites of pyrrolizidine alkaloids. Toxicon. 1989; 27:561. [PubMed: 2749755]
40. Zierer A, Melby SJ, Voeller RK, Moon MR. Interatrial shunt for chronic pulmonary hypertension: differential impact of low-flow versus high-flow shunting. Am J Physiol Heart Circ Physiol. 2009; 296:H639. [PubMed: 19136607]
41. Amirhamzeh MMR, Dean DA, Jia C, Cabreriza SE, Yano OJ, Burkhoff D, Spotnitz HM. Validation of right and left ventricular conductance and echocardiography for cardiac function studies. Ann Thorac Surg. 1996; 62:1104. [PubMed: 8823097]

42. Most P, Remppis A, Pleger ST, Löffler E, Ehlermann P, Bernotat J, Kleuss C, Heierhorst J, Ruiz P, Witt H, Karczewski P, Mao L, Rockman HA, Duncan SJ, Katus HA, Koch WJ. Transgenic overexpression of the Ca^{2+}-binding protein S100A1 in the heart leads to increased in vivo myocardial contractile performance. J Biol Chem. 2003; 278:33809. [PubMed: 12777394]
43. Quaile MP, Rossman EI, Berretta RM, Bratinov G, Kubo H, Houser SR, Margulies KB. Reduced sarcoplasmic reticulum Ca^{2+} load mediates impaired contractile reserve in right ventricular pressure overload. J Mol Cell Cardiol. 2007; 43:552. [PubMed: 17931654]
44. Rajkumar R, Konishi K, Richards TJ, Ishizawar DC, Wiechert AC, Kaminski N, Ahmad F. Genomewide RNA expression profiling in lung identifies distinct signatures in idiopathic pulmonary arterial hypertension and secondary pulmonary hypertension. Am J Physiol Heart Circ Physiol. 2010; 298:H1235. [PubMed: 20081107]
45. Verhaert D, Mullens W, Borowski A, Popovic ZB, Curtin RJ, Thomas JD, Tang WHW. Right ventricular response to intensive medical therapy in advanced decompensated heart failure. Circ Heart Fail. 2010; 3:340. [PubMed: 20176715]
46. Drake JI, Bogaard HJ, Mizuno S, Clifton B, Xie B, Gao Y, Dumur CI, Fawcett P, Voelkel NF, Natarajan R. Molecular signature of a right heart failure program in chronic severe pulmonary hypertension. Am J Respir Cell Mol Biol. 2011; 45:1239. [PubMed: 21719795]
47. Mizuno S, Bogaard HJ, Kraskauskas D, Alhussaini A, Gomez-Arroyo J, Voelkel NF, Ishizaki T. p53 Gene deficiency promotes hypoxia-induced pulmonary hypertension and vascular remodeling in mice. Am J Physiol Lung Cell Mol Physiol. 2011; 300:L753. [PubMed: 21335523]
48. Kogler H, Harmann O, Leineweber K, Nguyen vP, Schott P, Brodde OE, Hasenfuss G. Mechanical load-dependent regulation of gene expression in monocrotaline-induced right ventricular hypertrophy in the rat. Circ Res. 2003; 93:230. [PubMed: 12842921]
49. Bogaard HJ, Natarajan R, Henderson SC, Long CS, Kraskauskas D, Smithson L, Ockaili R, McCord JM, Voelkel NF. Chronic pulmonary artery pressure elevation is insufficient to explain right heart failure. Circulation. 2009; 120:1951. [PubMed: 19884466]
50. Michelakis ED, Wilkins MR, Rabinovitch M. Emerging concepts and translational priorities in pulmonary arterial hypertension. Circulation. 2008; 118:1486. [PubMed: 18824655]

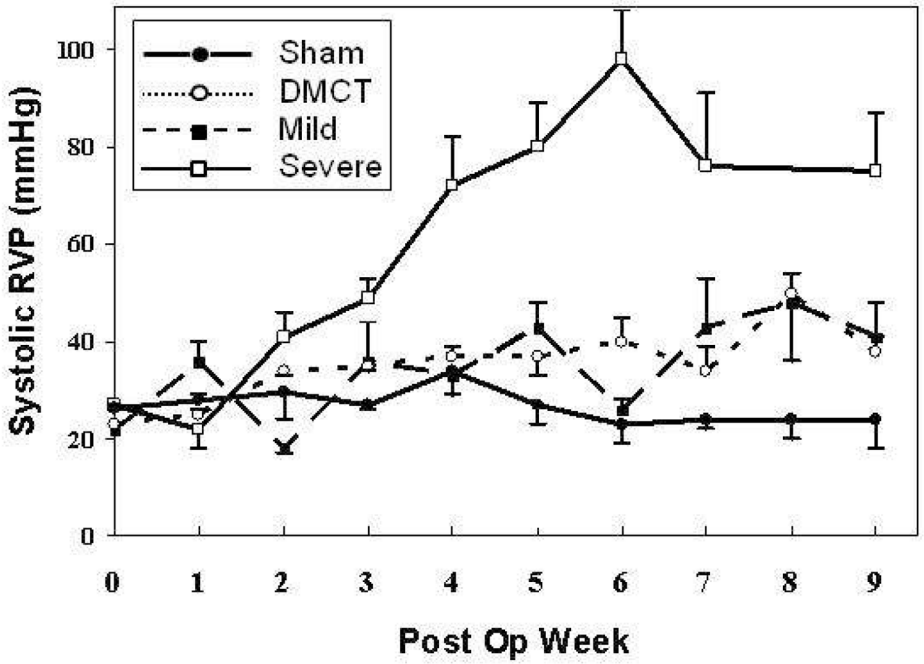

Figure 1.

Average weekly systolic right ventricular (RV) pressure measurements in the Sham (lower solid line, solid circle), dehydromonocrotaline (DMCT) (dotted line, open circle), mild pulmonary artery (PA) band (dashed line, solid square), and severe PA band (upper sold line, open square) groups. Error bars depict standard error of the mean at each time point.

2A

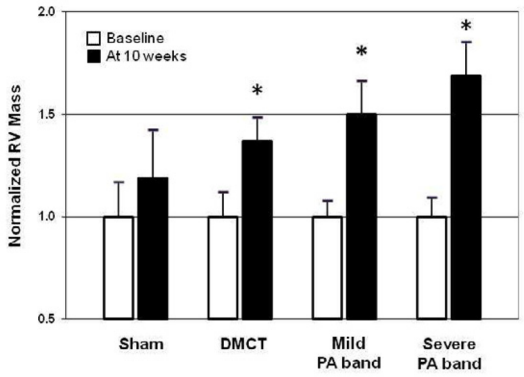

2B

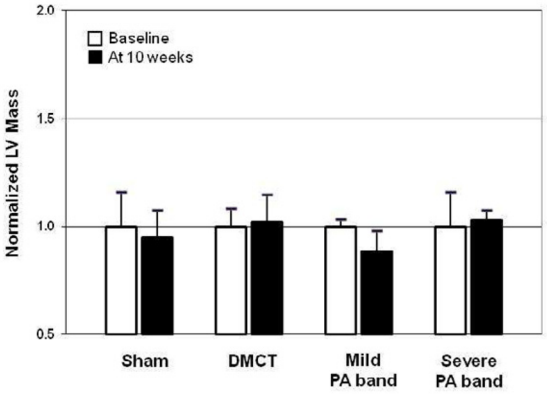

Figure 2.

A.) Right ventricular (RV) and B.) left ventricular (LV) mass normalized to baseline (white bars) and after 10 weeks (dark bars) in sham, dehydromonocrotaline (DMCT), mild pulmonary artery (PA) band, and severe PA band groups (mean ± one standard error, * $P < 0.05$ versus baseline).

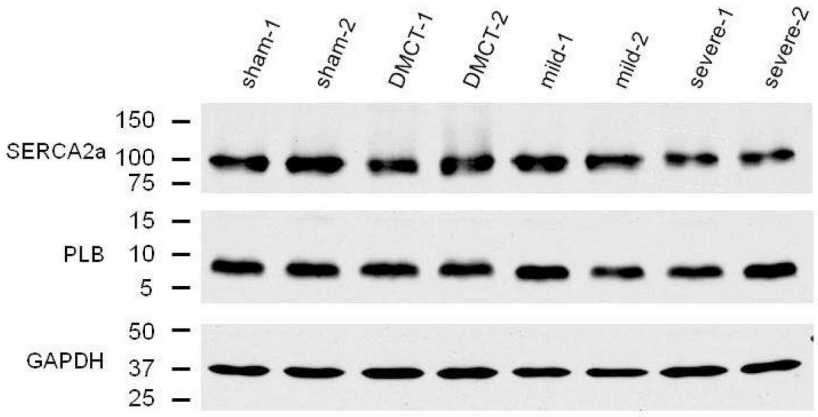

Figure 3.
Western blotting of right ventricular (RV) sarcoplasmic reticulum Ca^{2+}-ATPase (SERCA2a) and phospholamban (PLB) in sham, dehydromonocrotaline (DMCT), and mild and severe pulmonary artery (PA) band groups. These gels includes two typical dogs from each group.

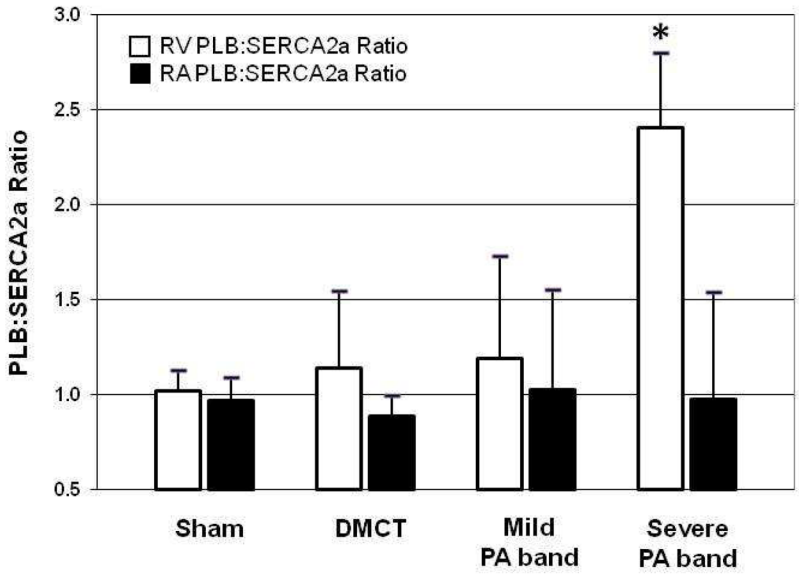

Figure 4.

The right ventricular (RV) PLB:SERCA2a protein ratio (normalized to GAPDH) increased with severe pulmonary artery (PA) band compared to sham operated controls, but there was no change with dehydromonocrotaline (DMCT) or mild PA band. The right atrial (RA) PLB:SERCA2a protein ratio did not change in any group. $*P < 0.05$.

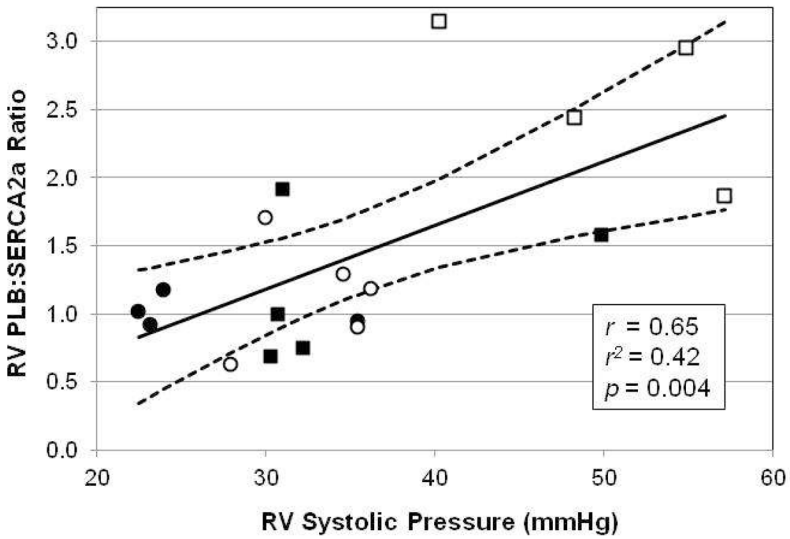

Figure 5.

Correlation of right ventricular (RV) PLB:SERCA2a protein ratio to systolic RV pressure measured in anesthetized, open-chest, closed-pericardium state. All 18 animals were included in this analysis, including sham (solid circles), dehydromonocrotaline (DMCT, open circles), mild pulmonary artery (PA) banding (solid squares), and severe PA banding (open squares). The solid line represents the predicted values from the linear regression PLB:SERCA2a = −0.22 + (0.47 × RVP), and the dashed lines represent 95% confidence intervals.

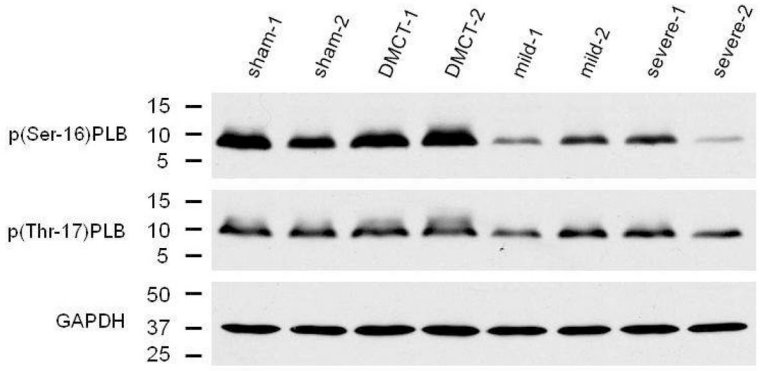

Figure 6.
Western blotting of right ventricular (RV) phosphorylation of phospholamban at amino acid serine-16 (p(Ser-16)PLB) and threonine-17 (p(Thr-17)PLB) in sham, dehydromonocrotaline (DMCT), and mild and severe pulmonary artery (PA) band groups. These gels includes two typical dogs from each group.

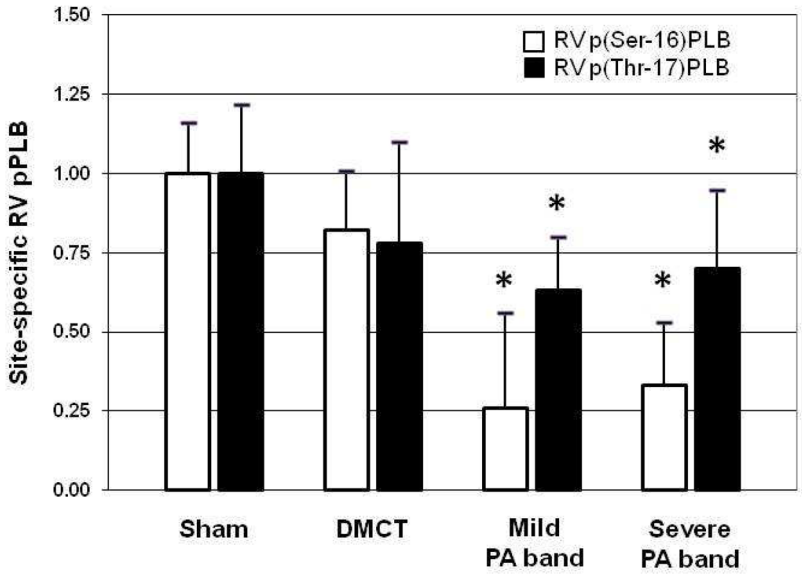

Figure 7.

Amino acid site-specific right ventricular (RV) phosphorylated phospholamban (pPLB). There was a tendency for pPLB to fall at both serine-16 and threonine-17 in the dehydromonocrotaline (DMCT) and mild and severe pulmonary artery (PA) band groups. $*P < 0.05$.

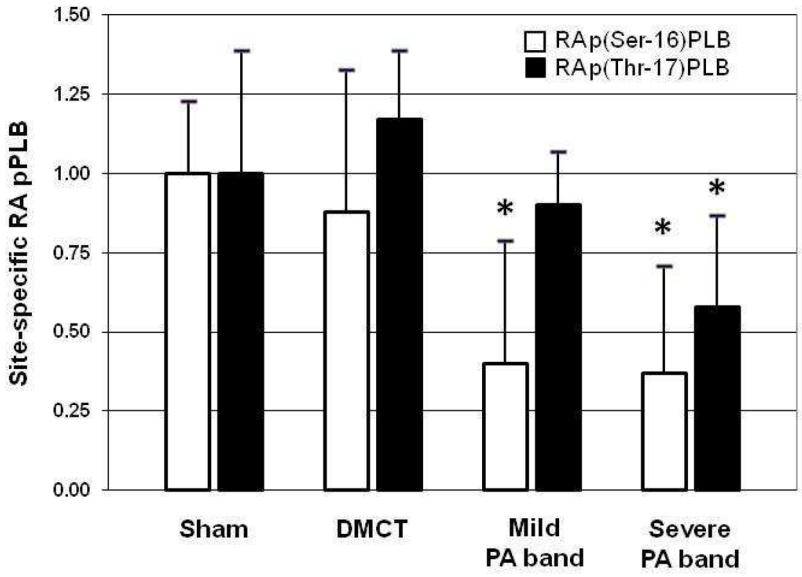

Figure 8.

Amino acid site-specific right atrial (RA) phosphorylated phospholamban (pPLB). There was a significant decline in RA pPLB at serine-16 in the pulmonary artery (PA) band groups and at threonine-17 in the severe PA band group, but there was no significant change in the dehydromonocrotaline (DMCT) group. $*P < 0.05$.

TABLE 1

Impact of dehydromonocrotaline (DMCT) toxicity mild and severe pulmonary artery (PA) banding on ventricular mass and hemodynamics

	Baseline	Sham (n=4)	DMCT (n=5)	Mild PA Band (n=5)	Severe PA Band (n=4)
Body weight (kg)		18.1 ± 0.4	19.9 ± 2.2	20.3 ± 0.9	20.1 ± 0.3
Heart rate (beats/min)	108 ± 13	108 ± 6	111 ± 10	100 ± 17	94 ± 15 *
Systolic RVP (mmHg)	26.9 ± 4.1	26.2 ± 6.1	32.8 ± 3.7 *	34.7 ± 8.5	50.0 ± 7.8 *
Mean RAP (mmHg)	6.0 ± 2.1	5.6 ± 3.1	7.9 ± 1.5 *	8.2 ± 2.1 *	7.9 ± 0.7 *
Mean LAP (mmHg)	8.0 ± 2.1	6.0 ± 2.2	7.5 ± 3.5	9.6 ± 3.4	9.7 ± 2.7
Cardiac output (L/min)	2.7 ± 0.6	2.7 ± 0.2	3.2 ± 1.0	2.4 ± 0.6	2.4 ± 0.6
RV dP/dt_{MAX} (mmHg/s)	364 ± 101	378 ± 97	415 ± 57	349 ± 64	452 ± 79
RV dP/dt_{MIN} (mmHg/s)	−328 ± 167	−386 ± 171	−389 ± 126	−351 ± 186	−431 ± 129
RV wall thickness (cm)	0.62 ± 0.13	0.62 ± 0.08	0.68 ± 0.14	0.80 ± 0.13 *	0.88 ± 0.28 *
RV FAS (%)	33 ± 23	35 ± 19	33 ± 35	29 ± 28	42 ± 19
RV wall stress (k×dynes/cm^2)	31.9 ± 9.3	30.9 ± 7.8	38.7 ± 14.1	45.7 ± 30.0	63.4 ± 25.4 *

dP/dt, rate of pressure change; FAS, fractional area shortening; LAP, left atrial pressure; LV, left ventricular; RAP, right atrial pressure; RV, right ventricular; RVP, right ventricular pressure. Data are mean ± standard deviation. Baseline data are pooled for all four groups in this table for clarity of presentation; however, statistical analyses were performed using group-specific baselines with two-way repeated measures analysis of variance and Fisher's LSD test.

* $P < 0.05$ versus group-specific Baseline.

TABLE 2

Impact of dehydromonocrotaline (DMCT) toxicity and mild and severe pulmonary artery (PA) banding on right ventricular and right atrial calcium-handling proteins

	Sham (n=4)	DMCT (n=5)	Mild PA Band (n=5)	Severe PA Band (n=4)
Right Ventricle:				
SERCA2a	1.00 ± 0.18	1.04 ± 0.09	0.78 ± 0.30	0.43 ± 0.18*
PLB	1.00 ± 0.10	1.19 ± 0.41	0.82 ± 0.19	0.84 ± 0.28
pPLB at serine-16	1.00 ± 0.16	0.82 ± 0.19	0.26 ± 0.30*	0.33 ± 0.20*
pPLB at threonine-17	1.00 ± 0.22	0.78 ± 0.32	0.63 ± 0.17*	0.70 ± 0.25*
Right Atrium:				
SERCA2a	1.00 ± 0.14	1.14 ± 0.10	1.07 ± 0.23	0.81 ± 0.26
PLB	1.00 ± 0.18	1.00 ± 0.07	0.97 ± 0.24	0.72 ± 0.28
pPLB at serine-16	1.00 ± 0.23	0.88 ± 0.44	0.40 ± 0.39*	0.37 ± 0.34*
pPLB at threonine-17	1.00 ± 0.39	1.17 ± 0.22	0.90 ± 0.17	0.58 ± 0.29*

PLB, phospholamban; pPLB, phosphorylated PLB; SERCA2a, sarcoplasmic reticulum Ca^{2+}-ATPase. Data are mean ± standard deviation normalized to GAPDH and Sham group.

* $P < 0.05$ versus Sham (ANOVA, Fisher's LSD test).